IEEE Access
Multidisciplinary | Rapid Review | Open Access Journal

SPECIAL SECTION ON KEY ENABLING TECHNOLOGIES FOR PROSUMER ENERGY MANAGEMENT

Received November 27, 2020, accepted December 8, 2020, date of publication December 16, 2020, date of current version January 5, 2021.

Digital Object Identifier 10.1109/ACCESS.2020.3045151

Integrated Optimal Dispatching Strategy Considering Power Generation and Consumption Interaction

ZHIGANG LIU[1,2], ZHENFENG XIAO[1,2], YEFAN WU[1,2], HUI HOU[3], (Member, IEEE), TAO XU[3], QINGYONG ZHANG[3], AND CHANGJUN XIE[3], (Member, IEEE)

[1]State Grid Hunan Electric Power Company Ltd. Economic and Technical Research Institute, Changsha 410007, China
[2]Hunan Key Laboratory of Energy Internet Supply-demand and Operation, Changsha 410004, China
[3]School of Automation, Wuhan University of Technology, Wuhan 430072, China

Corresponding author: Qingyong Zhang (qyzhang@whut.edu.cn)

This work was supported in part by the Science and Technology Project of State Grid Hunan Electric Power Company under Grant 5216A220000F, and in part by the Science-Technology Innovation Platform and Talents Program of Hunan Province, China, under Grant 2019TP1053.

ABSTRACT The rapid development of renewable energy and the continuous growth of peak load bring new challenges to the dispatching capacity of generation side. In view of the possible mismatch between power generation of renewable energy and the load, we propose an integrated optimal dispatching strategy model of power generation and consumption interaction in this paper. Among them, the generation side resources include wind power, photovoltaic and battery energy storage and the load side dispatching resources include transferable load, interruptible load and electric vehicles. The model takes the benefits of generation side and the benefits of load side as objectives. Moreover, three different dispatching orders are put forward, which are random dispatching, interruption and transfer of load before electric vehicles charging and discharging, electric vehicles charging and discharging before interruption and transfer of load. In addition, we propose seven different dispatching combinations based on the optimal dispatching order to analyse the response ability of different load side dispatching resources. Multi-objective Genetic Algorithm and the method of technique for order preference by similarity to an ideal solution are applied in this study to obtain the optimal results. It can be identified that the response ability of different load side dispatching resources is different, and the overall dispatching can improve the benefits of generation side and the benefits of load side. Meanwhile, the proposed strategy considers the willingness of the load to the greatest extent and effectively improves the utilization rate of wind and solar power generation.

INDEX TERMS Generation side resources, load side dispatching resources, integrated optimal dispatching, dispatching order, dispatching combination.

I. INTRODUCTION

With more and more renewable energy such as wind power and photovoltaic are connected to the power grid [1], there are still some problems in the process of dispatching generation side (GS) resources, such as insufficient peak regulation capacity, serious wind and solar abandonment [2]–[4]. In recent years, the rapid development of adjustable load and electric vehicles (EVs) provides abundant load side dispatching resources (LSDRs), which brings an opportunity to improve the problems encountered in the process of GS dispatching [5], [6]. Therefore, considering the interaction of wind power, photovoltaic, battery energy storage, adjustable load and EVs is the main trend to improve the matching relationship between renewable energy and load.

At present, scholars have carried out some research on the integrated optimal dispatching of power generation and consumption interaction. Munoz *et al.* [7] established a two stage decision-making model of ''day-ahead and real-time'' to coordinate the optimization of renewable energy and load side (LS) resources on two time scales. Parvania *et al.* [8] proposed the model of transferable load (TL) and applied it to the day-ahead optimal economic dispatching model with wind farm. The model improved the flexibility of dispatching.

The associate editor coordinating the review of this manuscript and approving it for publication was Bin Zhou.

Similarly, Qiu *et al.* [9] proposed a generation dispatching model, which considered the cost of interruptible load (IL). The model took the economic optimization of power grid as the objective function. The results showed that the proposed model was more robust to random changes and could be flexibly dispatched in power generation dispatching. In addition, considering the mobile energy storage characteristics of EVs, Chen *et al.* [10] proposed a dispatching strategy for mobile energy storage of EVs in collaboration with renewable energy. The strategy analysed the charging and discharging of EVs to dispatch. Liu *et al.* [11] established a source-load coordination economic dispatch model with the goal of maximizing wind power consumption and minimizing the operation cost of the system. In the above research on the integrated optimal dispatching strategy considering power generation and consumption interaction, most of them are limited to consider the single LSDRs. At the same time, they seldom consider the influence of the participation of EVs, TL and IL on the resource dispatching of GS.

In the study of integrated optimal dispatching considering power generation and consumption interaction, the LSDRs have different response capacity and response characteristics at different times, which can optimize the load curve and promote the consumption of renewable energy [12], [13]. Sun *et al.* [14] established the model of TL and IL. It was verified that the dispatching of adjustable load can adjust the load curve reasonably and realize the economic operation of the system. Considering the transfer of cooling load, heating load and electric load, Hu *et al.* [15] constructed a multi-objective optimization model. The model considered the factors of economic, energy and environmental, and optimized the load curve reasonably. In addition, Ju *et al.* [16] designed four strategies based on the error characteristics of wind power and the dispatching potential of load in multi-time. It made full use of the load resources under multi-time and effectively improved the wind power consumption level. Boulanger *et al.* [17] concentrated a large number of EVs together to improve the charging and discharging capacity of EVs. In order to optimize the load curve, the EVs were dispatched in a cluster mode. The above studies provided a good theoretical basis for the analysis of the response characteristics of LSDRs.

To sum up, most of the existing studies focused on the response capacity of single LSDRs, and did not fully reflect the response capacity of different combinations of LSDRs. Besides, there are few comparative studies on different LSDRs participating in dispatching. Compared with the existing studies, the major contributions of this paper can be summarized as:

1) An integrated optimal dispatching model of power generation and consumption interaction is established. Among them, the GS resources include wind power, photovoltaic and battery energy storage. The LSDRs include TL, IL and EVs.
2) An integrated optimal dispatching strategy is proposed. In the strategy, in order to encourage the LSDRs to better respond to the dispatching, the LS declares electricity price itself when participating in dispatching.
3) Considering the dispatching orders of various LSDRs, the dispatching results under different dispatching orders are compared. Based on the optimal dispatching order, the dispatching results of different combinations are compared to analyze the response ability of different LSDRs.

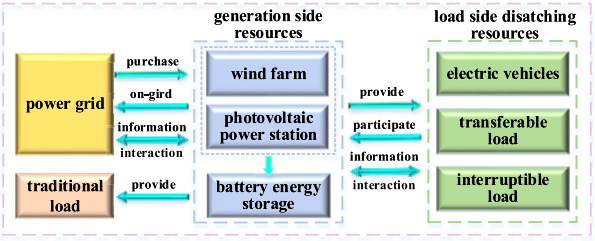

FIGURE 1. The integrated structure of power generation and consumption interaction.

The rest of this paper is organized as follows: mathematical models of power generation and consumption resources are given in Section 2. In Section 3, the integrated optimal dispatching strategy model of power generation and consumption interaction is established. Results and analysis of simulation are discussed in Section 4. Then conclusions are drawn in Section 5.

II. MATHEMATICAL MODELS OF POWER GENERATION AND CONSUMPTION RESOURCES

The integrated structure of power generation and consumption interaction is shown in Figure 1. It is mainly composed of photovoltaic power station, wind farm, battery energy storage, TL, IL, EVs and traditional load. This section mainly establishes the resource model of each part.

A. MODEL OF WIND TURBINE

In wind farm, the output of wind turbine is determined by the wind speed and the output characteristics of wind turbine. The power of wind turbine is calculated by [18]:

$$P_{\mathrm{w}}(v) = \begin{cases} 0, & v \le v_{\mathrm{in}} \\ \dfrac{v^3 - v_{\mathrm{in}}^3}{v_{\mathrm{r}}^3 - v_{\mathrm{in}}^3} P_{\mathrm{r}}, & v_{\mathrm{in}} \le v \le v_{\mathrm{r}} \\ P_{\mathrm{r}}, & v_{\mathrm{r}} \le v \le v_{\mathrm{out}} \\ 0, & v \ge v_{\mathrm{out}} \end{cases} \tag{1}$$

where, $P_{\mathrm{w}}(v)$ is the power of wind turbine, P_{r} is the rated power, v_{in} is the cut-in wind speed, v_{out} is the cut-out wind speed, v_{r} is the rated wind speed, v is the wind speed at the corresponding time.

B. MODEL OF PHOTOVOLTAIC CELL

The output power of photovoltaic array is strongly nonlinear, which is related to solar radiation intensity and ambient temperature. The following simplified model can be used and the

power of photovoltaic cell is calculated by [19]:

$$P_{\mathrm{p}} = f_{\mathrm{p}} Y_{\mathrm{p}} \frac{I_{\mathrm{T}}}{I_{\mathrm{S}}} \left[1 + \alpha_{\mathrm{p}} \left(T_{\mathrm{c}} - T_{\mathrm{c,STC}}\right)\right] \tag{2}$$

where, f_{p} is the derating factor of photovoltaic array, which represents the ratio of actual output power of photovoltaic array to rated output power, Y_{p} is the output power of battery under standard test conditions (the illumination is 1kW/m^2, ambient temperature is 25°C, no wind), I_{T} is the solar radiation intensity of photovoltaic panel, I_{S} is the illumination under standard test conditions with a value of 1kW/m^2, α_{p} is the power temperature coefficient, T_{c} is the operating temperature of the battery board, $T_{\mathrm{c,STC}}$ is the reference temperature.

C. MODEL OF BATTERY ENERGY STORAGE

The battery is used as the energy storage system in this paper. The charging and discharging of the battery energy storage can be expressed by Eqs. (3) and (4) [20].

(1) When the battery energy storage is charged, $P_{\mathrm{bes}}(t) \geq 0$, the quantity of electric charge at time t is

$$E_{\mathrm{bes}}(t) = E_{\mathrm{bes}}(t-1) + P_{\mathrm{bes}}(t)\,\eta_{\mathrm{besc}} \tag{3}$$

(2) When the battery energy storage is discharged, $P_{\mathrm{bes}}(t) \leq 0$, the quantity of electric charge at time t is

$$E_{\mathrm{bes}}(t) = E_{\mathrm{bes}}(t-1) + P_{\mathrm{bes}}(t)/\eta_{\mathrm{besd}} \tag{4}$$

where, $E_{\mathrm{bes}}(t)$ is the quantity of electric charge of battery energy storage at time t, $P_{\mathrm{bes}}(t)$ is the charging and discharging power of battery energy storage at time t, η_{besc} and η_{besd} are the charging and discharging efficiency of battery energy storage, respectively.

In order to prevent the battery energy storage from overcharging and discharging, the remaining energy of battery energy storage should be kept within a certain range.

$$SOC_{\min} \leq SOC(t) \leq SOC_{\max} \tag{5}$$

where, $SOC(t)$ is the state of charge of battery energy storage at time t, $SOC_{\min}$ and $SOC_{\max}$, respectively, are the upper and lower limits of the state of charge of battery energy storage with values of 0.5 and 0.9.

D. MODEL OF TL

The TL is that the users change the load of electricity consumption period according to the electricity price or incentive measures. In the load transfer mode, the users don't need to reduce the living needs or interrupt the production task and only need to change the time of power use. The total power consumption is kept unchanged during the period, so that the living demand and total production will not be affected. However, the power consumption of each period can be flexibly adjusted within a certain range [6].

In the process of participating in GS dispatching, this paper considers to transfer the unimportant load whose load is greater than wind and solar power to the period when the load is less than wind and solar power. And the time when the load is less than the wind and solar power does not belong to the peak period. After load transfer, the load of each period is the original load plus the increased load, and then the reduced load is reduced.

$$P^{\mathrm{tr}}_{\mathrm{Lafter}}(t) = P_{\mathrm{L}}(t) + P^{\mathrm{tr}}_{\mathrm{u}}(t) - P^{\mathrm{tr}}_{\mathrm{d}}(t) \tag{6}$$

where, $P^{\mathrm{tr}}_{\mathrm{Lafter}}(t)$ is the total load after load transfer at time t, $P_{\mathrm{L}}(t)$ is the original load, $P^{\mathrm{tr}}_{\mathrm{u}}(t)$ is the increased load at time t, $P^{\mathrm{tr}}_{\mathrm{d}}(t)$ is the reduced load at time t.

In the dispatching process, it is necessary to ensure that the total load after transfer is not greater than the wind and solar power, and the transfer period is the period when the load is greater than the wind and solar power. At the same time, the total amount of TL before and after transfer should be kept unchanged in a certain period of time. The constraints are shown in Eqs. (7) ∼ (10).

$$P^{\mathrm{tr}}_{\mathrm{Lafter}}(t) \leq P_{\mathrm{wt}}(t) + P_{\mathrm{pv}}(t) \tag{7}$$

$$P^{\mathrm{tr}}_{\min} \leq |P^{\mathrm{trl}}(t) - P^{\mathrm{trb}}(t)| \leq P^{\mathrm{tr}}_{\max} \tag{8}$$

$$t^{\mathrm{tr}}_{\min} \leq t \leq t^{\mathrm{tr}}_{\max} \tag{9}$$

$$\sum_{t=1}^{24} P^{\mathrm{trb}}(t) = \sum_{t=1}^{24} P^{\mathrm{trl}}(t) \tag{10}$$

where, $P_{\mathrm{wt}}(t)$ and $P_{\mathrm{pv}}(t)$ are wind power and photovoltaic power at time t, respectively; $P^{\mathrm{trb}}(t)$ and $P^{\mathrm{trl}}(t)$ are the total TL before and after transferring at time t respectively; $P^{\mathrm{tr}}_{\min}$ and $P^{\mathrm{tr}}_{\max}$, respectively, are the upper and lower limits of the total TL; $t^{\mathrm{tr}}_{\min}$ and $t^{\mathrm{tr}}_{\max}$, respectively, are the upper and lower limits of the transferable time.

E. MODEL OF IL

The IL is the load that can be interrupted during peak period or emergency. It refers to the implementation of load interruption operation in specific period, such as peak load period, according to the interruption contract signed in advance. It is a kind of demand response mode that makes certain economic compensation to the users who perform interrupt operation after the event [21].

When the load is greater than the wind and solar power, the load interruption is executed. After the interruption, the load of each period is the original load minus the interrupted load.

$$P^{\mathrm{in}}_{\mathrm{Lafter}}(t) = P_{\mathrm{L}}(t) - P^{\mathrm{in}}_{\mathrm{d}}(t) \tag{11}$$

where, $P^{\mathrm{in}}_{\mathrm{Lafter}}(t)$ is the total load after load interruption at time t, $P^{\mathrm{in}}_{\mathrm{d}}(t)$ is the load interrupted at time t.

Similarly, the upper and lower limits of IL and interruptible time are constrained.

$$P^{\mathrm{in}}_{\min} \leq P^{\mathrm{in}}(t) \leq P^{\mathrm{in}}_{\max} \tag{12}$$

$$t^{\mathrm{in}}_{\min} \leq t \leq t^{\mathrm{in}}_{\max} \tag{13}$$

where, $P^{\mathrm{in}}(t)$ is the total IL at time t, $P^{\mathrm{in}}_{\min}$ and $P^{\mathrm{in}}_{\max}$, respectively, are the upper and lower limits of the total IL; $t^{\mathrm{in}}_{\min}$ and $t^{\mathrm{in}}_{\max}$, respectively, are the upper and lower limits of the interruptible time.

F. MODEL OF EVS

The survey results of the U.S. Department of transportation on U.S. household vehicles in 2001 were statistically analysed in [22], and the return time of the last journey of the vehicles was approximately normal distribution. The starting charging time is the return time of the last journey, so the starting charging time satisfies the normal distribution. Its probability density function is shown in Eq (14).

$$f_t(t) = \begin{cases} \dfrac{1}{\sigma_t\sqrt{2\pi}} \exp\left[\dfrac{-(t-\mu_t)^2}{2\sigma_t^2}\right] \\ \qquad\qquad (\mu_t - 12) < t \leq 24 \\ \dfrac{1}{\sigma_t\sqrt{2\pi}} \exp\left[\dfrac{-(t+24-\mu_t)^2}{2\sigma_t^2}\right] \\ \qquad\qquad 0 < t \leq (\mu_t - 12) \end{cases} \tag{14}$$

where, $\mu_t = 17.6$, $\sigma_t = 3.4$.

EVs are limited by users' driving habits. In the process of participating in GS dispatching, the starting time of charging and discharging of EVs is determined by analyzing the relationship between return time of EVs, wind and solar power and load.

When $P_{\mathrm{L}}(t_0) \leq P_{\mathrm{wt}}(t_0) + P_{\mathrm{pv}}(t_0)$,

$$T_{\mathrm{char}} = t_0 \tag{15}$$

When $P_{\mathrm{L}}(t_0) \geq P_{\mathrm{wt}}(t_0) + P_{\mathrm{pv}}(t_0)$,

$$T_{\mathrm{dischar}} = t_0 \tag{16}$$

where, T_{char} is the starting time of EVs charging and T_{dischar} is the starting time of EVs discharging.

$$SOC_{\mathrm{EV\,min}} \leq SOC_{\mathrm{EV}}(t) \leq SOC_{\mathrm{EV\,max}} \tag{17}$$

where, $SOC_{\mathrm{EV}}(t)$ is the state of charge of EVs at time t, $SOC_{\mathrm{EV\,min}}$ and $SOC_{\mathrm{EV\,max}}$, respectively, are the upper and lower limits of the state of charge of EVs with values of 20% and 90%.

III. THE INTEGRATED OPTIMAL DISPATCHING STRATEGY MODEL

A. THE INTEGRATED OPTIMAL DISPATCHING STRATEGY

The integrated dispatching strategy considering power generation and consumption interaction proposed in this paper is to integrate the LSDRs into the dispatching process of the GS, so as to realize the overall optimization of the power generation and consumption resources. The specific dispatching process is shown in Figure 2.

The dispatching process of GS includes two cases: wind and solar power is greater than load and wind and solar power is less than load. When the wind and solar power is greater than load, in addition to the conventional load, there is residual power. After integrating into the LSDRs, the remaining power dispatching includes on-grid, battery energy storage charging, EVs charging, etc. Based on the time-of-use electricity price, if the price of power grid is the peak time price, it is on-grid. If the price of power grid is the valley time price, the battery energy storage will be charged and a certain number of EVs will be selected for charging.

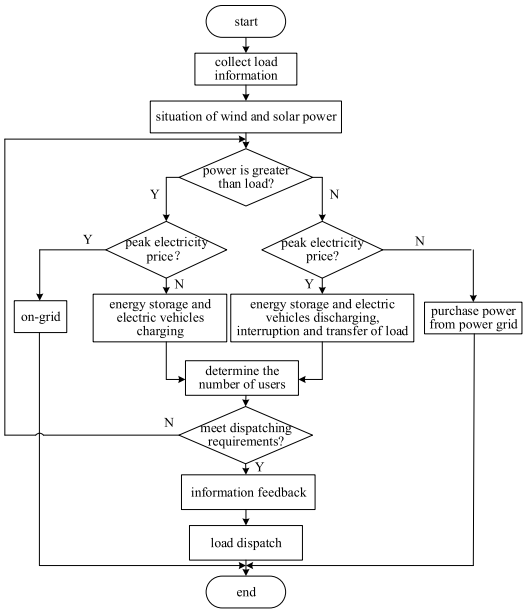

FIGURE 2. The integrated optimal dispatching of power generation and consumption interaction process.

When the wind and solar power is less than the load, the dispatching mode includes power purchasing from power grid, battery energy storage discharging, EVs discharging and interruption and transfer of load. These modes can be used for the insufficient part after supplying the conventional load. Based on the time-of-use electricity price, if the price of power grid is valley time price, it will be purchased from power grid. If the price of power grid is peak time price, the battery energy storage will be discharged. If it is not enough, a certain number of EVs will be selected for discharge and the load will be interrupted and transferred.

If the dispatching requirements are met, the above dispatching information will be fed back to the LS, and the LS will respond according to the feedback information. In order to encourage the LSDRs to better respond to the dispatching, the LS is compensated by reducing or increasing the electricity price. That is to say, the LSDRs will quote itself when participating in the dispatching, but it should be in line with the actual situation and cannot be quoted at will. Therefore, the dispatching process is based on the following assumptions: 1) In order to avoid random declaring the price on the LS, the declaring is carried out within a certain range, but the real-time price mechanism in the electricity market is not considered. 2) In order to simplify the calculation, the unified declaration is selected. In other words, based on the time-of-use electricity price, the declared price of TL and EVs charging is 0.9 times of the time-of-use electricity price. The declared price of IL and EVs discharge is 1.2 times of time-of-use electricity price [23]. 3) A certain number of LSDRs are preset to participate in the dispatching, but not all of them are involved in the actual dispatching. 4) For the LSDRs, the electricity declared by each user remains constant. 5) Lithium

battery electric vehicle is selected as the dispatching object, and the impact of short-term charging or discharging on it can be ignored. Based on the above-mentioned model of EVs, when the EVs arrive, it will be charged and discharged for 1 hour within the range of the state of charge.

B. OBJECTIVE FUNCTION OF THE MODEL

Based on the above-mentioned dispatching strategy, a dispatching strategy model is established with the objective functions of maximizing the benefits of GS and maximizing the benefits of LS.

(1) Objective function 1: the maximum benefits of GS. It includes the benefits of power supplied by wind farm, photovoltaic power station and battery energy storage to the LS, the benefits of on-grid, power purchasing cost and operation and maintenance cost.

$$F_1 = \max[C_U + C_G - C_C - C_O] \tag{18}$$

$$C_U = \sum_{t=1}^{24}\sum_{i=1}^{4}(-1)^{i+1}p_i^*(t)c_i^*(t) + \sum_{t=1}^{24}p(t)c_b(t) \tag{19}$$

$$C_G = \sum_{t=1}^{24}p_b(t)c_b(t) \tag{20}$$

$$C_C = \sum_{t=1}^{24}p_m(t)c_m(t) \tag{21}$$

$$C_O = \Delta t_{wt}\cdot C_{wt}^{om} + \Delta t_{pv}\cdot C_{pv}^{om} + \Delta t_{bes}\cdot C_{bes}^{om} \tag{22}$$

where, F_1 is the benefits of GS, C_U is the benefits of power supplied by wind farm, photovoltaic power station and battery energy storage to the LS, C_G is the benefits of on-grid, C_C is power purchasing cost, C_O is operation and maintenance cost, $p_i^*(t)$ is the type i load participating in dispatching at time t (1 is transfer of load, 2 is interruption of load, 3 is EVs charging and 4 is EVs discharging), $p(t)$ is the load that does not participate in the dispatching, $p_b(t)$ is the on-grid power at time t, $p_m(t)$ is the amount of power purchased from power grid at time t, $c_i^*(t)$ is the declared electricity price of the type i load participating in dispatching at time t, $c_b(t)$ is the on-grid price at time t, $c_m(t)$ is the price of electricity purchased at time t, Δt_{wt}, Δt_{pv} and Δt_{bes} are the operation time of wind farm, photovoltaic power station and battery energy storage in one day, respectively; C_{wt}^{om}, C_{pv}^{om} and C_{bes}^{om} are the operation and maintenance cost of wind farm, photovoltaic power station and battery energy storage in unit time, respectively.

(2) Objective function 2: the maximum benefits of LS, which is the difference of power consumption cost before and after dispatching.

$$F_2 = \max[C_B - C_A] \tag{23}$$

$$C_B = \sum_{t=1}^{24}P_L(t)c_b(t) \tag{24}$$

$$C_A = \sum_{t=1}^{24}\sum_{i=1}^{4}p_i^*(t)c_i^*(t) + \sum_{t=1}^{24}p(t)c_b(t) \tag{25}$$

where, F_2 is the benefits of LS, C_B is the power cost of LS before dispatching, C_A is the power cost of LS after dispatching.

C. CONSTRAINT CONDITION

The constraints of the optimal dispatching strategy model are as follows:

(1) In order to ensure a certain utilization rate of wind and solar power, the ratio of the power provided by the wind and solar to the load is used to reflect the utilization rate of wind and solar power generation (UR).

$$R = \sum_{t=1}^{24}E(t)/\sum_{t=1}^{24}P_L^*(t) \geq R_r \tag{26}$$

where, R is the UR, $E(t)$ is the amount of power provided to load by wind and solar power at time t, $P_L^*(t)$ is the load after dispatching at time t, R_r is the rated UR with a value of 0.5.

(2) In order to avoid excessive peak shift during dispatching, which leads to "peak on peak", and to avoid excessive load fluctuation before and after dispatch, load variance is constrained.

$$\mu \leq \mu_a \tag{27}$$

$$\mu = [\sum_{t=1}^{24}(\sum_{i=1}^{4}p_i^*(t) + p(t) - P_a)^2]/24 \tag{28}$$

$$P_a = \sum_{t=1}^{24}(\sum_{i=1}^{4}p_i^*(t) + p(t))/24 \tag{29}$$

where, μ is the load variance, μ_a is the rated load variance, P_a is the average load after dispatching.

(3) Satisfaction with electricity price expenditure (SEPE) is used to describe satisfaction evaluation of the load' price expenditure after responding to the dispatching.

$$s \leq s_r \tag{30}$$

$$s = 1 - \frac{[\sum_{t=1}^{24}\sum_{i=1}^{4}p_i^*(t)c_i^*(t) + \sum_{t=1}^{24}p(t)c_b(t)] - \sum_{t=1}^{24}P_L(t)c_b(t)}{\sum_{t=1}^{24}P_L(t)c_b(t)} \tag{31}$$

where, s is the SEPE, s_r is the rated satisfaction with a value of 1.

(4) Other constraints.

$$s.t.\ (5), (7) - (10), (12) - (13), (17) \tag{32}$$

D. SOLUTION METHOD

In this paper, the multi-objective genetic algorithm (NSGA) [24], [25] is used to solve the model. A series of non-inferior solutions can be obtained by using NSGA and the Pareto Front is composed of a series of non-inferior solutions. Then, the optimal solution is determined in the Pareto Front by technique for order preference by similarity to an ideal solution (TOPSIS) [26]. TOPSIS is an effective

method commonly used in solving multi-objective problems. Its basic principle is to sort by judging the distance between the evaluation object and the optimal solution and the most split. The TOPSIS is described as follows:

If there are m evaluation objects (a series of non-inferior solutions) and n evaluation indexes (the objective functions), then there is decision matrix $X = (x_{ij})_{m\times n}$. Where x_{ij} represents the value of the i-th evaluation object in the j-th evaluation index. And $M = \{1, 2, \ldots, m\}, N = \{1, 2, \ldots, n\}$.

Step 1: Construct the normalized decision matrix $Y = (y_{ij})_{m\times n}$.

$$y_{ij} = \frac{x_{ij}}{\sqrt{\sum_{i=1}^{m} x_{ij}^2}} \tag{33}$$

Step 2: Assign weights to the evaluation indexes to construct a weighted standardized decision matrix $Z = (z_{ij})_{m\times n}$, the matrix elements are

$$z_{ij} = w_j y_{ij} \tag{34}$$

where, w_j is the weight of the j-th evaluation index.

Step 3: Determine the positive and negative ideal solutions A^+ and A^-.

$$\begin{cases} A^+ = (z_1^+, z_2^+, \ldots, z_n^+) \\ A^- = (z_1^-, z_2^-, \ldots, z_n^-) \end{cases} \tag{35}$$

$$z_j^+ = \max_i z_{ij}, z_j^- = \min_i z_{ij} \tag{36}$$

Step 4: Calculate the Euclidean distances d_i^+ and d_i^- between each evaluation object and the positive and negative ideal solutions.

$$d_i^+ = \|z_i - A^+\| = \sqrt{\sum_{j=1}^{n} \left(z_{ij} - z_j^+\right)^2} \tag{37}$$

$$d_i^- = \|z_i - A^-\| = \sqrt{\sum_{j=1}^{n} \left(z_{ij} - z_j^-\right)^2} \tag{38}$$

where, z_i is the i-th row of the weighted normalized decision matrix, corresponding to the j-th evaluation object.

Step 5: Calculate the posting progress of each evaluation object and the positive ideal solution.

$$C_i^+ = \frac{d_i^-}{d_i^+ + d_i^-} \tag{39}$$

It can be seen from Eq. (39) that when C_i^+ approaches 1, the evaluation object is close to the positive ideal solution.

Step 6: Sort C_i^+ in descending order. According to the ranking, the result closest to the ideal solution is the optimal evaluation object, that is, the optimal benefits in this paper.

The specific calculation process is shown in Figure 3.

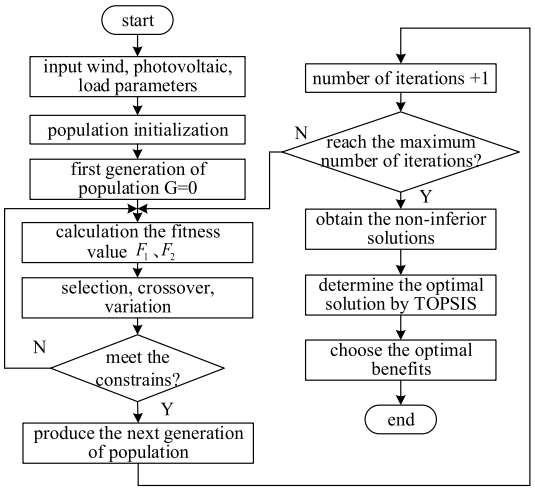

FIGURE 3. The calculation process of dispatching strategy model.

IV. RESULTS AND ANALYSIS

A. SIMULATION PARAMETERS

This paper focuses on the influence of different dispatching sequences and dispatching combinations on the integrated dispatching strategy of power generation and consumption interaction. Therefore, the impact of load uncertainty on the dispatching strategy is not considered, only from the existing model and historical data. The load curve is shown in Figure 4. Referring to the relevant data of a certain area (105.0° E, 35.4° N), it can be seen from the China Meteorological Data Service Center that the average illumination is 4.32 kW/m2 and the average wind speed is 4.87 m/s. The forecast data of wind speed and illumination in a day can be obtained in the HOMER software [27]. The curves of wind and solar power are obtained by using the power calculation formula, which are shown in Figure 5 and Figure 6.

The capacities of wind farm, photovoltaic power station, battery energy storage are 120 MW, 160 MW and 30 MW, respectively. For the TL and IL, the power declared by each user is 0.2 MW, and the charging and discharging power of EVs are both 30 kW. This paper presupposes that the number of TL users participating in the declaration is 100, the number of IL users is 100, and the number of EVs is 4000. In addition, time-of-use electricity price is adopted for

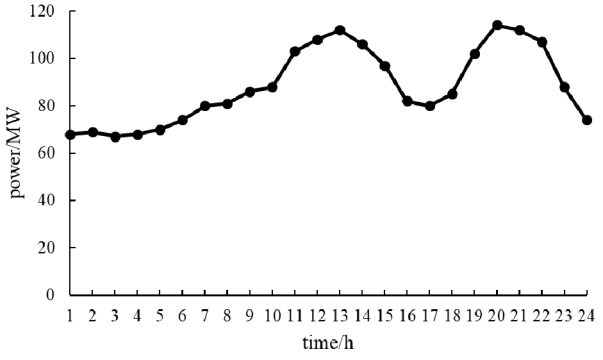

FIGURE 4. The original load curve.

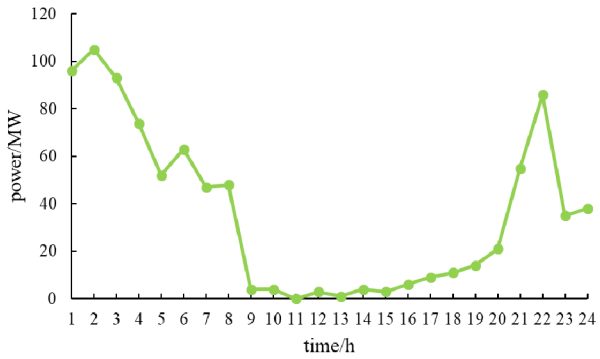

FIGURE 5. The wind power curve.

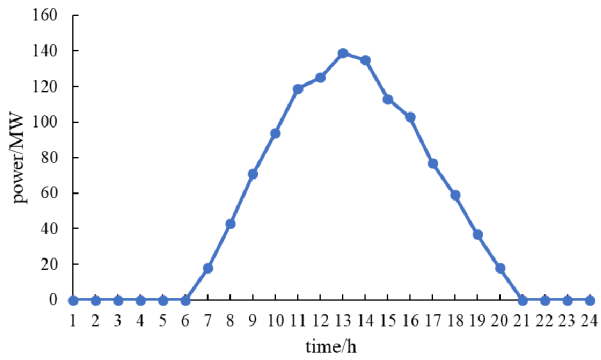

FIGURE 6. The solar power curve.

TABLE 1. On-Grid electricity price and purchase electricity price.

time	price/(￥/(MW·h))	
	on-grid	purchase
peak period(10:00-15:00, 18:00-21:00)	650	830
flat period(07:00-10:00, 15:00-18:00, 21:00-23:00)	380	490
valley period(23:00-07:00)	130	170

TABLE 2. Operation and maintenance costs of GS resources.

	operation and maintenance costs
wind farm	29.6￥/MW·h
photovoltaic power station	9.6￥/MW·h
battery energy storage	9.0￥/MW·h

both on-grid electricity price and electricity purchasing price from power grid [28], as shown in Table 1. The operation and maintenance costs of wind farm, photovoltaic power station and battery energy storage are shown in Table 2 [29].

In the process of dispatching, the different orders and combinations of LSDRs participating in dispatching will affect the results. In order to analyze the influence of different dispatching orders and dispatching combinations of TL, IL and EVs on the integrated dispatching strategy considering power generation and consumption interaction, three different dispatching orders are proposed, which are: Order 1: random dispatching (without considering the order of three kinds of LSDRs); Order 2: interruption and transfer of load before EVs charging and discharging; Order 3: EVs charging and discharging before interruption and transfer of load. In addition, seven different dispatching combinations are proposed, which are random permutation and combination of three LSDRs, as shown in Table 3.

TABLE 3. Seven different dispatching combinations.

combination	TL	IL	EVs
1	+	+	+
2	+	+	
3	+		+
4		+	+
5	+		
6		+	
7			+

TABLE 4. The optimal solutions under three dispatching orders.

	benefits of GS (￥)	benefits of LS (￥)
before dispatching	790 900	—
order 1	777 366	31 613
order 2	798 486	22 521
order 3	779 221	20 669

TABLE 5. The total number of LSDRS under three dispatching orders.

	IL	TL	EVs
order 1	58	94	1 552
order 2	61	68	1 397
order 3	55	79	1 078

B. RESULTS AND ANALYSIS UNDER DIFFERENT DISPATCHING ORDERS

Taking into account the uncertainty of LSDRs, such as TL, IL and EVs, Monte Carlo method [30] is used to simulate the electricity consumption behavior of users. The NSGA is used to solve the Pareto Front of the benefits of the GS and the benefits of the LS under three different dispatching orders, as shown in Figure 7 (a), (b) and (c).

The optimal solutions under three dispatching orders are determined in the Pareto Front by TOPSIS, which are shown in Table 4. In addition, the total number of LSDRs under three dispatching orders are shown in Table 5.

It can be seen from Table 4 and Table 5 that the benefits of LS is the largest, but the benefits of GS is the smallest under order 1. It shows that more users participate in the dispatching under order 1, which is more flexible for users to participate in dispatching and effectively improves the benefits of LS. However, in order to compensate for IL and EVs discharge, part of the benefits of GS is lost. However, for the order 3, the benefits of LS is the smallest and the benefits of GS is increased by 0.24% compared to order 1. It shows that the

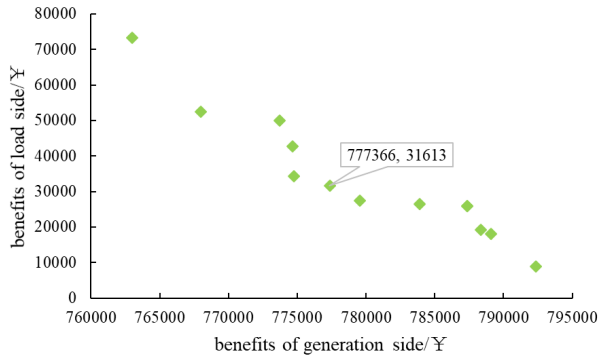

(a) Pareto Front under order 1

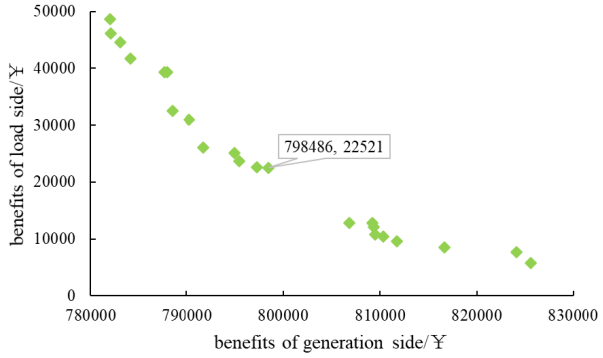

(b) Pareto Front under order 2.

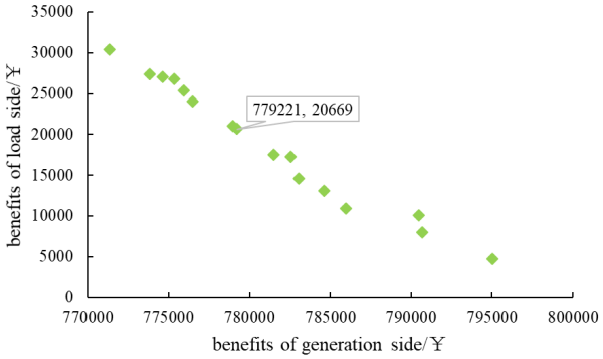

(c) Pareto Front under order 3.

FIGURE 7. Pareto Front under three different dispatching orders.

dispatching results are not ideal under order 3, which not only does not attract more users to participate in the dispatching, but also reduces the benefits of GS. The results show that different dispatching orders have a certain impact on the dispatching results and the number of users participating in the scheduling plays a major role.

In addition, the load curves under three dispatching orders are shown in Figure 8. The SEPE and the UR are shown in Figure 9.

It can be seen from Figure 8 that the fluctuation of load curve under order 1 is the minimum, that is, the load variance is the minimum. The original load is optimized to a certain extent. The second is order 2 and the last is order 3. In addition, it can be seen from Figure 9 that SEPE and the UR are optimal under order 1. It shows that when more users participate in the dispatching process, it can maximize the satisfaction of users, and make full use of wind and

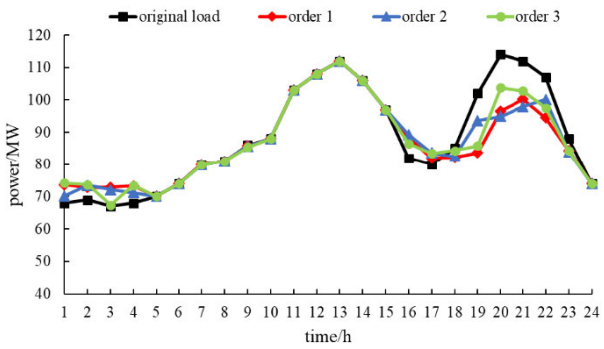

FIGURE 8. The load curves under three dispatching orders.

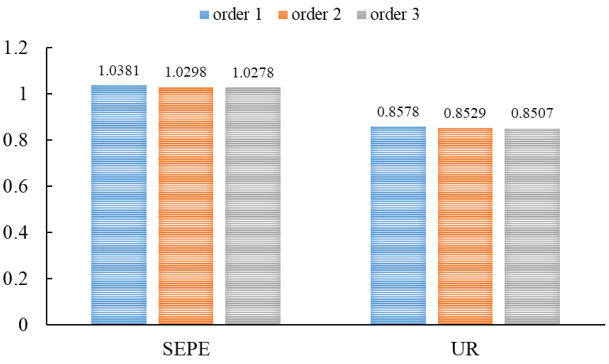

FIGURE 9. Indexes comparison under three dispatching orders.

solar resources, which improves the level of wind and solar consumption. To sum up, order 1 is the optimal dispatching strategy among the three different dispatching orders.

C. RESULTS AND ANALYSIS UNDER ORDER 1

The above conclusions show that order 1 is the optimal, so the results of order 1 are analyzed in detail. The number of TL arranged at each moment is shown in Table 6. The number of IL arranged at each moment is shown in Table 7. The number of EVs arranged at each moment is shown in Table 8, where the number of charging is positive and the number of discharging is negative.

It can be seen from Table 6 to Table 8 that the number of the LSDRs is different at each moment under the order 1. Due to the limitation of driving habits, the number of EVs participating in dispatching at each moment is quite different, but the EVs participating in dispatching can meet the normal travel demand.

TABLE 6. The number of TL.

time	1	2	3	4
number	23	17	28	26

TABLE 7. The number of IL.

time	19	20	21	22
number	17	21	12	8

TABLE 8. The number of EVS.

time	1	2	3	4	5	6	7	8
number	36	15	11	3	0	0	-1	0
time	9	10	11	12	13	14	15	16
number	-5	0	0	0	0	0	0	209
time	17	18	19	20	21	22	23	24
number	67	-95	-346	-327	-125	-189	-123	0

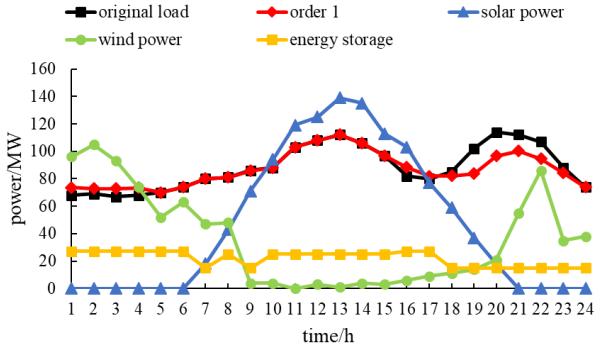

FIGURE 10. The load curves under order 1.

The load curve under order 1 is shown in Figure 10. In the low load period, wind resources are sufficient and the wind power is greater than the load, while in the late peak period, the wind power is less than the load. After dispatching, part of the load in the late peak period is transferred to the low period, which plays a role of ''peak cutting and valley filling'' to the original load to a certain extent. From 01:00 to 03:00, the wind power generation is sufficient. From 11:00 to 16:00, the solar power generation is sufficient. In addition to meeting the load demand, the excess power is connected to power grid. The energy storage chooses to discharge in the period of high electricity price, so there are only a few discharges in the dispatching process. However, due to the peak load at night, the wind power generation is not enough to supply the load demand, so the power is purchased from the power gird.

In addition, the power curves of LSDRs participating in the dispatching is shown in Figure 11. The optimal dispatching strategy transfers part of the load from 19:00-22:00 to 01:00-04:00 and interrupts part of the load from 19:00 to 22:00. The dispatching of EVs is more flexible. In the low period and 16:00-17:00, the wind and solar power generation is sufficient. The EVs are charged, and the electricity price is low during the low period, which can save the charging cost. However, in the late peak period, the EVs begin to discharge, which not only relieves the pressure of peak power consumption, but also obtains the benefits.

D. RESULTS AND ANALYSIS UNDER DIFFERENT DISPATCHING COMBINATIONS

In order to analyze the response ability of different LSDRs, different dispatching combinations are studied based on the order 1. The NSGA is used to solve the Pareto Front of the benefits of the GS and the benefits of the LS

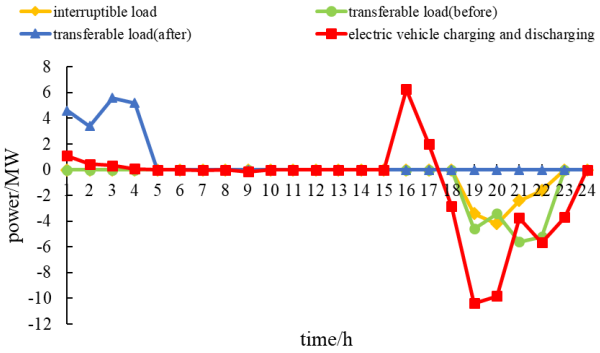

FIGURE 11. The power curves of LSDRs.

TABLE 9. The optimal solutions under seven dispatching combinations.

	benefits of GS (￥)	benefits of LS (￥)
combination 1	777 366	31 613
combination 2	787 313	8 330
combination 3	796 836	26 279
combination 4	791 655	16 937
combination 5	793 544	9 061
combination 6	788 305	1 300
combination 7	793 382	14 723

under seven different dispatching combinations, as shown in Figure 12 (a), (b), (c), (d), (e) and (f). The optimal solutions under seven dispatching combinations are determined in the Pareto Front by TOPSIS, which are shown in Table 9.

It can be seen from Table 9 that the benefits of LS is the largest under combination 1, but the benefits of GS is the smallest. It shows that the participation of various LSDRs can effectively improve the benefits of LS, but the benefits of GS is damaged because of the large number of participation.

For combinations 2 and 6, IL participates in dispatching, which makes the benefits of GS less. This is mainly because of the need for price compensation for IL. At the same time, the benefits of LS is small, which indicates that the number of IL participating in dispatching is less. It indirectly indicates that few users participate in load interruption. For combinations 2, 3 and 5 with TL, the benefits of GS is great, and the LS also has certain benefits. The main reason is that the load is transferred from the peak time price to the valley time price. While stimulating the load transfer, the GS loses part of the benefits, but the GS gets the balance in other aspects. Besides, in addition to combination 1, the benefits of LS of combinations 3, 4 and 7 are larger. The common point is that EVs participate in the dispatching, which makes the dispatching more flexible and effectively improves the benefits of LS.

The load curves under seven dispatching combinations are shown in Figure 13. The SEPE and the UR are shown in Figure 14.

It can be seen from Figure 13 that the load curve fluctuation under combination 1 is the smallest. For combinations 2, 3 and 4, there are two kinds of LSDRs participating in the

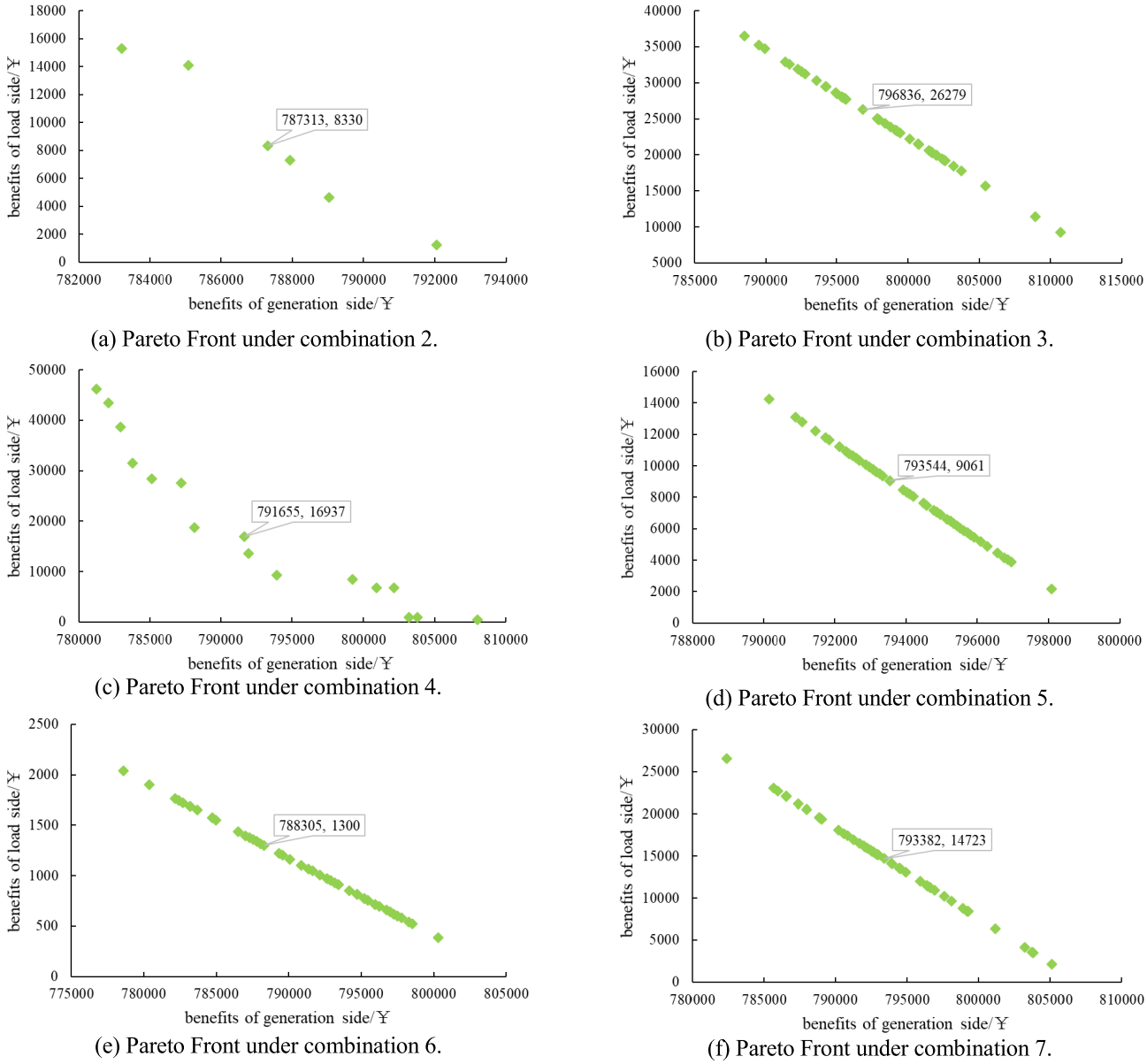

(a) Pareto Front under combination 2.

(b) Pareto Front under combination 3.

(c) Pareto Front under combination 4.

(d) Pareto Front under combination 5.

(e) Pareto Front under combination 6.

(f) Pareto Front under combination 7.

FIGURE 12. Pareto Front under seven different dispatching combinations.

dispatching, so the load curve fluctuations are smaller than that of combinations 5, 6 and 7. At the same time, the load curve fluctuation of combination 3 is the smallest, followed by combinations 2 and 4, which shows that the TL has the best effect in reducing the load curve fluctuation, followed by EVs and IL. In addition, for combinations 5, 6, and 7, the load curve fluctuation of combination 5 is the smallest, followed by combinations 7, 6. The same conclusion is obtained.

It can be seen from Figure 14 that the SEPE and the UR under combination 1 are optimal. Similarly, for combinations 2, 3 and 4 with two kinds of LSDRs, the SEPE and the UR are better than those of combinations 5, 6 and 7. For combinations 2, 3 and 4, the SEPE and the UR under combination 3 are optimal, followed by combinations 4 and 2. Similarly, for combinations 5, 6 and 7, the SEPE and the UR under combination 7 are optimal, followed by combinations 5 and 6. The results show that EVs can maximize the satisfaction of users participating in dispatching, and has the best effect in the use of wind and solar resources. The second is the TL and the last is the IL.

In conclusion, EVs, as a mobile energy storage unit, can not only charge but also discharge. It can effectively utilize the wind and solar resources and improve the level of wind and solar energy consumption. Meanwhile, TL can effectively reduce the load curve fluctuation. Therefore, EVs and TL should be selected first in the integrated optimal dispatching process of power generation and consumption interaction.

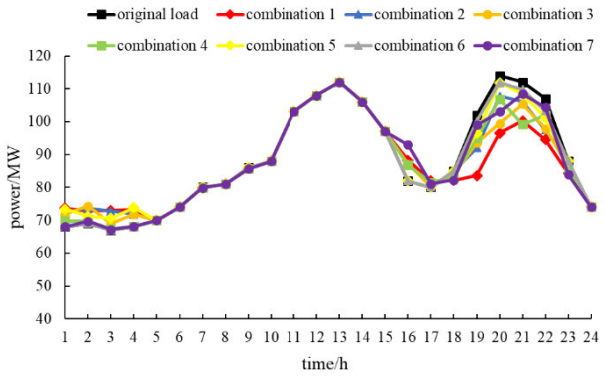

FIGURE 13. The load curves under seven dispatching combinations.

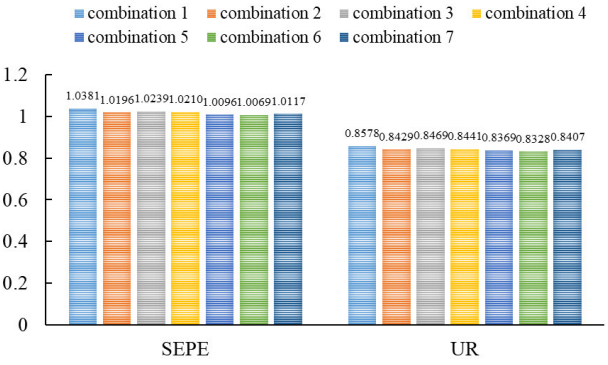

FIGURE 14. Indexes comparison under seven dispatching combinations.

The IL can increase the reserve resources in the peak load period, and as an auxiliary in the dispatching process, it can optimize the dispatching results.

V. CONCLUSION

In this paper, an integrated optimal dispatching strategy of power generation and consumption interaction is proposed. The GS resources include wind power, photovoltaic and battery energy storage. The LSDRs include TL, IL and EVs. By comparing three different dispatching orders, the results without considering the order of three kinds of LSDRs are optimal. Furthermore, seven different dispatching combinations are compared based on the optimal dispatching order, which verifies that the dispatching strategy considers the willingness of the LS to the greatest extent and effectively improves the UR. At the same time, it plays a role of ''peak cutting and valley filling'' to the original load to a certain extent. Therefore, in the future, EVs and TL should be selected first in the integrated optimal dispatching process of power generation and consumption interaction and IL should be used as auxiliary in the dispatching process, which can optimize the dispatching results.

It should be pointed out that, in this study, the unified declaration of electricity price is taken without considering the diversity of declaration. Therefore, further studies will focus on the diversity of declaration of electricity price and the diversity of LSDRs participating in dispatching.

REFERENCES

[1] S. Xia, Z. Ding, T. Du, D. Zhang, M. Shahidehpour, and T. Ding, ''Multi-time scale coordinated scheduling for the combined system of wind power, photovoltaic, thermal generator, hydro pumped storage, and batteries,'' *IEEE Trans. Ind. Appl.*, vol. 56, no. 3, pp. 2227–2237, May 2020.

[2] Y. Zeng, R. Zhang, D. Wang, Y. Mu, and H. Jia, ''A regional power grid operation and planning method considering renewable energy generation and load control,'' *Appl. Energy*, vol. 237, pp. 304–313, Mar. 2019.

[3] G. Yuan and W. Yang, ''Study on optimization of economic dispatching of electric power system based on hybrid intelligent algorithms (PSO and AFSA),'' *Energy*, vol. 183, pp. 926–935, Sep. 2019.

[4] D. Zhang, J. Wang, Y. Lin, Y. Si, C. Huang, J. Yang, B. Huang, and W. Li, ''Present situation and future prospect of renewable energy in China,'' *Renew. Sustain. Energy Rev.*, vol. 76, pp. 865–871, Sep. 2017.

[5] A. Triviño-Cabrera, J. A. Aguado, and S. D. L. Torre, ''Joint routing and scheduling for electric vehicles in smart grids with V2G,'' *Energy*, vol. 175, pp. 113–122, May 2019.

[6] H. Hou, M. Xue, Y. Xu, Z. Xiao, X. Deng, T. Xu, P. Liu, and R. Cui, ''Multi-objective economic dispatch of a microgrid considering electric vehicle and transferable load,'' *Appl. Energy*, vol. 262, Mar. 2020, Art. no. 114489.

[7] E. G. Munoz, G. G. Alcaraz, and N. G. Cabrera, ''Two-phase short-term scheduling approach with intermittent renewable energy resources and demand response,'' *IEEE Latin Amer. Trans.*, vol. 13, no. 1, pp. 181–187, Jan. 2015.

[8] M. Parvania, M. Fotuhi-Firuzabad, and M. Shahidehpour, ''Optimal demand response aggregation in wholesale electricity markets,'' *IEEE Trans. Smart Grid*, vol. 4, no. 4, pp. 1957–1965, Dec. 2013.

[9] J. Qiu, J. Zhao, and D. Wang, ''Multi-objective generation dispatch considering the trade-off between economy and security,'' *IET Gener., Transmiss. Distrib.*, vol. 12, no. 3, pp. 633–642, Sep. 2017.

[10] Z. Chen, Y. Liu, X. Chen, T. Zhou, and Q. Xing, ''Charging and discharging dispatching strategy for electric vehicles considering characteristics of mobile energy storage,'' *Autom. Electr. Power Syst.*, vol. 44, no. 2, pp. 77–88, 2020.

[11] W. Liu, J. Wen, C. Xie, W. Wang, and C. Liang, ''Multi-objective optimal method considering wind power accommodation based on source-load coordination,'' *Proc. CSEE*, vol. 35, no. 5, pp. 1079–1088, 2015.

[12] X. Lu, K. Zhou, X. Zhang, and S. Yang, ''A systematic review of supply and demand side optimal load scheduling in a smart grid environment,'' *J. Cleaner Prod.*, vol. 203, pp. 757–768, Dec. 2018.

[13] D. Wang, Q. Hu, H. Jia, K. Hou, W. Du, N. Chen, X. Wang, and M. Fan, ''Integrated demand response in district electricity-heating network considering double auction retail energy market based on demand-side energy stations,'' *Appl. Energy*, vol. 248, pp. 656–678, Aug. 2019.

[14] C. Sun, L. Wang, and H. Xu, ''An interaction load model and its application in microgrid day-ahead economic scheduling,'' *Power Syst. Technol.*, vol. 40, no. 7, pp. 2009–2016, 2016.

[15] R. Hu, M. Zhang, and L. I. Zhenkun, ''Optimal operation for CCHP system considering shiftable loads,'' *Power Syst. Technol.*, vol. 42, no. 3, pp. 715–721, 2018.

[16] L. Ju, Q. Tan, H. Lin, S. Mei, N. Li, Y. Lu, and Y. Wang, ''A two-stage optimal coordinated scheduling strategy for micro energy grid integrating intermittent renewable energy sources considering multi-energy flexible conversion,'' *Energy*, vol. 196, Apr. 2020, Art. no. 117078.

[17] A. G. Boulanger, A. C. Chu, S. Maxx, and D. L. Waltz, ''Vehicle electrification: Status and issues,'' *Proc. IEEE*, vol. 99, no. 6, pp. 1116–1138, Jun. 2011.

[18] J. Chen, F. Wang, and K. A. Stelson, ''A mathematical approach to minimizing the cost of energy for large utility wind turbines,'' *Appl. Energy*, vol. 228, pp. 1413–1422, Oct. 2018.

[19] Y. Zhang, K. Meng, F. Luo, H. Yang, J. Zhu, and Z. Y. Dong, ''Multi-agent-based voltage regulation scheme for high photovoltaic penetrated active distribution networks using battery energy storage systems,'' *IEEE Access*, vol. 8, pp. 7323–7333, 2020.

[20] D. Rosewater, S. Ferreira, D. Schoenwald, J. Hawkins, and S. Santoso, ''Battery energy storage state-of-charge forecasting: Models, optimization, and accuracy,'' *IEEE Trans. Smart Grid*, vol. 10, no. 3, pp. 2453–2462, May 2019.

[21] F.-C. Gu, S.-D. Lu, J.-X. Wu, C.-L. Kuo, C.-H. Lin, and S.-J. Chen, ''Interruptible power estimation and auxiliary service allocation using contract theory and dynamic game for demand response in aggregator business model,'' *IEEE Access*, vol. 7, pp. 129975–129987, 2019.

[22] L. Tian, S. Shi, and Z. Jia, "A statistical model for charging power demand of electric vehicles," *Power Syst. Technol.*, vol. 34, no. 11, pp. 126–130, Nov. 2010.
[23] Y. Luo, Y. Xue, G. Ledwich, Z. Y. Dong, H. Liu, and W. Hu, "Coordination of low price interruptible load and high compensation interruptible load," *Autom. Electr. Power Syst.*, vol. 31, no. 11, pp. 17–21, 2007.
[24] C. Han, L. Wang, Z. Zhang, J. Xie, and Z. Xing, "A multi-objective genetic algorithm based on fitting and interpolation," *IEEE Access*, vol. 6, pp. 22920–22929, 2018.
[25] J. Bonilla, L. J. Yebra, S. Dormido, and E. Zarza, "Parabolic-trough solar thermal power plant simulation scheme, multi-objective genetic algorithm calibration and validation," *Sol. Energy*, vol. 86, no. 1, pp. 531–540, Jan. 2012.
[26] F. Cavallaro, "Fuzzy TOPSIS approach for assessing thermal-energy storage in concentrated solar power (CSP) systems," *Appl. Energy*, vol. 87, no. 2, pp. 496–503, Feb. 2010.
[27] A. Sagani, G. Vrettakos, and V. Dedoussis, "Viability assessment of a combined hybrid electricity and heat system for remote household applications," *Sol. Energy*, vol. 151, pp. 33–47, Jul. 2017.
[28] M. Miao, L. Yong, and C. Yijia, "Optimization strategy of muti-energy hybrid AC/DC power system considering environmental factors," *Autom. Electr. Power Syst.*, vol. 42, no. 4, pp. 128–134, 2018.
[29] M. Ding, B. Wang, B. Zhao, Z. N. Chen, "Configuration optimization of capacity of standalone PV-wind-diesel-battery hybrid microgrid," *Power Syst. Technol.*, vol. 37, no. 3, pp. 575–581, 2013.
[30] X. Li, Z. Liu, Y. Tang, X. Gao, Y. Ma, and S. Tao, "Reliability analysis of the security and stability control device based on the Monte Carlo method," *Energy Procedia*, vol. 145, pp. 9–14, Jul. 2018.

ZHIGANG LIU is currently the Vice Dean of the State Grid Hunan Electric Power Company Ltd. Economic and Technical Research Institute, Changsha, China. He is also a Senior Engineer and an Expert in the field of optimal dispatching and safe operation with Power Grid. His research interests include dispatching and operation of power grid, and power grid intelligence.

ZHENFENG XIAO received the Ph.D. degree in electrical engineering from Wuhan University, Wuhan, China, in 2014.

He is currently an Engineer with the State Grid Hunan Electric Power Company Ltd. Economic and Technical Research Institute, Changsha, China. His research interests include control and protection of microgrid, and optimal planning of smart grid.

YEFAN WU received the M.S. degree from Hunan University, Changsha, China.

He is currently an Engineer with the State Grid Hunan Electric Power Company Ltd. Economic and Technical Research Institute, Changsha. His research interests include power system control and automation, and optimal planning of smart grid.

HUI HOU (Member, IEEE) was born in Wuhan, Hubei, China, in May 1981. She received the B.S. degree from Wuhan University, Wuhan, in 2003, and the Ph.D. degree from the Huazhong University of Science and Technology, Wuhan, in 2009.

She is currently an Associate Professor with the School of Automation, Wuhan University of Technology. Her research interests include the energy Internet and integrated energy systems.

TAO XU received the B.S. degree from the School of Automation, Wuhan University of Technology, Wuhan, China, in 2018, where he is currently pursuing the M.S. degree.

His research interests include energy storage, and distributed generation planning and operation.

QINGYONG ZHANG received the M.S. and Ph.D. degrees from the Wuhan University of Technology, Wuhan, China, in 2009 and 2020, respectively.

She is currently an Associate Professor with the School of Automation, Wuhan University of Technology. Her research interests include intelligent optimization and control, multi-objective optimization, and machine learning.

CHANGJUN XIE (Member, IEEE) received the Ph.D. degree in vehicle engineering from the Wuhan University of Technology (WHUT), Wuhan, China, in 2009.

From 2012 to 2013, he was a Visiting Scholar with the University of California at Davis, Davis, CA, USA. He is currently a Professor with the School of Automation, WHUT, Wuhan. He is also the Vice Dean of the School of Automation, WHUT. He has published over 50 articles, and over 40 articles are indexed by SCI or EI. His research interests include control strategy of fuel cell vehicles, intelligent and connected vehicle, and vehicle control and optimization of new energy vehicles.